Palaeogeography, Palaeoclimatology, Palaeoecology 442 (2016) 61–71

Contents lists available at ScienceDirect

Palaeogeography, Palaeoclimatology, Palaeoecology

journal homepage: www.elsevier.com/locate/palaeo

The first fossil record of ring-cupped oak (*Quercus* L. subgenus *Cyclobalanopsis* (Oersted) Schneider) in Tibet and its paleoenvironmental implications

He Xu [a,c], Tao Su [a,d,*], Shi-Tao Zhang [e], Min Deng [f], Zhe-Kun Zhou [a,b,*]

[a] Key Laboratory of Tropical Forest Ecology, Xishuangbanna Tropical Botanical Garden, Chinese Academy of Sciences, Mengla 666303, China
[b] Key Laboratory for Plant Diversity and Biogeography of East Asia, Kunming Institute of Botany, Chinese Academy of Sciences, Kunming 650204, China
[c] University of Chinese Academy of Sciences, Beijing 100049, China
[d] State Key Laboratory of Paleobiology and Stratigraphy, Nanjing Institute of Geology and Paleontology, Chinese Academy of Sciences, Nanjing 210008, China
[e] Faculty of Land Resource Engineering, Kunming University of Science and Technology, Kunming 650093, China
[f] Shanghai Chengshan Plant Science Research Center, Chinese Academy of Sciences, Shanghai 201602, China

ARTICLE INFO

Article history:
Received 1 March 2015
Received in revised form 13 November 2015
Accepted 17 November 2015
Available online 02 December 2015

Keywords:
Cyclobalanopsis
Leaf
Miocene
Paleoclimate
Qinghai–Tibetan Plateau
Uplift

ABSTRACT

Some taxa are good indicators of particular climates because their distribution is determined by specific temperature or precipitation requirements. Ring-cupped oaks (*Quercus* L. subgenus *Cyclobalanopsis* (Oersted) Schneider) are mainly distributed in tropical and subtropical climates in southeastern and eastern Asia. Recently, we collected many leaf fossils of ring-cupped oaks from the Upper Miocene Lawula Formation of eastern Tibet at an elevation of 3910 m. No modern species of ring-cupped oaks could survive at such a high elevation under current climate conditions. Based on detailed morphological comparisons with extant and fossil species, we propose a new species, *Quercus tibetensis* H. Xu, T. Su et Z.K. Zhou sp. nov., representing the first fossil record of ring-cupped oaks in Tibet. We investigated the climate requirements of the nearest living relatives (NLRs) of *Q. tibetensis*, and the ranges of mean annual temperature (MAT) and mean annual precipitation (MAP) are 7.9 °C to 21.7 °C, and 733.0 mm to 2536.8 mm, respectively, compared with the current climate at the fossil site with MAT of 4.4 °C and MAP of 516.5 mm. The NLRs of *Q. tibetensis* are distributed at elevations from 70 m to 3000 m, much lower than the fossil locality (3910 m). The altitudinal difference of the fossil site is 161 m to 3091 m between the late Miocene and today, even considering the warmer global climate during the late Miocene. Our results indicate that the climate conditions at the fossil site during the late Miocene were warmer and more humid than the current climate. Meanwhile, this new fossil finding corroborates results from previous studies that the southeastern part of the Qinghai–Tibetan Plateau experienced continued uplift since the late Miocene.

1. Introduction

The uplift of the Qinghai–Tibetan Plateau is one of the most important geological events in the Cenozoic (Rowley, 1996) because it drastically changed the topography of Asia and contributed to global cooling (Raymo and Ruddiman, 1992). Researchers from many disciplines have focused on this region, but the timing and phases of the uplift of the Qinghai–Tibetan Plateau are still unresolved (Tapponnier et al., 2001; Harrison and Yin, 2004; Royden et al., 2008; Molnar et al., 2010; Wang et al., 2014). Previous studies have suggested that the Indian Plate began to collide with the Eurasian Plate approximately 56 Ma (Zhang et al., 2012) or 50 Ma ago (Molnar et al., 2010; Meng et al., 2012), and the southern Qinghai–Tibetan Plateau rose during the Paleogene (Rowley and Currie, 2006; Ding et al., 2014). The Neogene was a period of global cooling, intensification of the Asian monsoon (An et al., 2001; Zachos et al., 2008; Molnar et al., 2010; Miao et al., 2012; Tang et al., 2013), and continued uplift of the Qinghai–Tibetan Plateau (England and Houseman, 1989; Molnar et al., 1993; Zhang et al., 2004; Wu et al., 2008). Eastern Tibet is situated in the core region of the Qinghai–Tibetan Plateau, but the paleoenvironmental change that occurred there during the Neogene remains largely unknown.

Plant fossils have been widely used to reconstruct paleoenvironments in deep time, because their morphology and distribution are greatly shaped by the surrounding environments (Wing and Greenwood, 1993; Wolfe, 1995; Mosbrugger and Utescher, 1997; Tiffney and Manchester, 2001; Jordan, 2011). The taxonomic occurrences of specific plant fossils from the Qinghai–Tibetan Plateau can

* Corresponding authors at: Key Laboratory of Tropical Forest Ecology, Xishuangbanna Tropical Botanical Garden, Chinese Academy of Sciences, Mengla 666303, China.
E-mail addresses: sutao@xtbg.org.cn (T. Su), zhouzk@xtbg.ac.cn (Z.-K. Zhou).

http://dx.doi.org/10.1016/j.palaeo.2015.11.014
0031-0182/

shed light on paleoenvironmental change in the Qinghai–Tibetan Plateau (Xu et al., 1973; Spicer et al., 2003; Fang et al., 2006; Zhou et al., 2007; Song et al., 2010; Wang et al., 2013; Jacques et al., 2014). Paleobotanic studies have yielded important evidence for Neogene paleoenvironmental changes in Tibet. Xu et al. (1973) found Pliocene leaf fossils of *Quercus semicarpifolia* (*Q.* section *Heterobalanus*) between modern elevations of 5700–5900 m on the northern slope of Xixabangma Peak in southern Tibet. By using the maximum elevation limits of the nearest living relatives (NLRs) of *Q. semicarpifolia*, Xu et al. (1973) suggested that Xixabangma Peak has risen approximately 3000 m since the Pliocene. Spicer et al. (2003) used enthalpy calculated from an assemblage of leaf fossils from the Namling Basin, southern Tibet, and they found that Namling Basin reached its present elevation during the middle Miocene. Song et al. (2010) used the Coexistence Approach with pollen occurrence data to estimate the paleoelevation of the Gangdise–Nyainqentanglha area in southern Tibet from the Eocene to the Holocene. They reported an Eocene elevation between 3295 and 3495 m and a Miocene elevation of 3000–3150 m. However, Neogene megafloral occurrences are rare in Tibet because of frequent and intensive Neogene deformation.

Ring-cupped oaks belong to *Quercus* subgenus *Cyclobalanopsis* (Fagaceae) and are often found in tropical and subtropical regions of southeast and east Asia (Fig. 1; Soepadmo, 1972; Huang et al., 1999; Luo and Zhou, 2001). Fossil leaves, acorns, cupules and wood of *Q.* subgenus *Cyclobalanopsis* are reported from Japan and China as early as the Eocene (Huzioka and Takahasi, 1970), but no fossils of ring-cupped oaks have previously been found in Tibet. Recently, we found many leaf fossils of ring-cupped oaks in late Miocene strata of Mangkang County, eastern Tibet at 3910 m.a.s.l. where no extant ring-cupped oaks survive today. This finding enhances our knowledge of the evolutionary diversification of *Q.* subgenus *Cyclobalanopsis* and provides further evidence about the paleoenvironmental change that has taken place in Tibet since the late Miocene.

Our discovery from a high elevation site in Mangkang is the first fossil record of ring-cupped oaks in Tibet, and is outside the modern climate range of extant ring-cupped oaks. We described the morphology of this new fossil species in detail and determined the environmental ranges of its NLRs to discuss the paleoclimate and paleoelevation of the southeastern Qinghai–Tibetan Plateau.

2. Materials and methods

2.1. Geological setting

The fossil site is located in Kajun village, about 16 km northwest of Gatuo Town in Mangkang County, eastern Tibet, China (29°45′10″N, 098°25′58″E; 3910 m a.s.l.; Fig. 1). The fossil bearing layer belongs to the Lawula Formation, which consists of interbedded mudstones and sandstones (Tao and Du, 1987). Fossil materials were collected from mudstones in the lower part of the Lawula Formation. Detailed information on the stratigraphy of the Lawula Formation has been extensively described in Su et al. (2014).

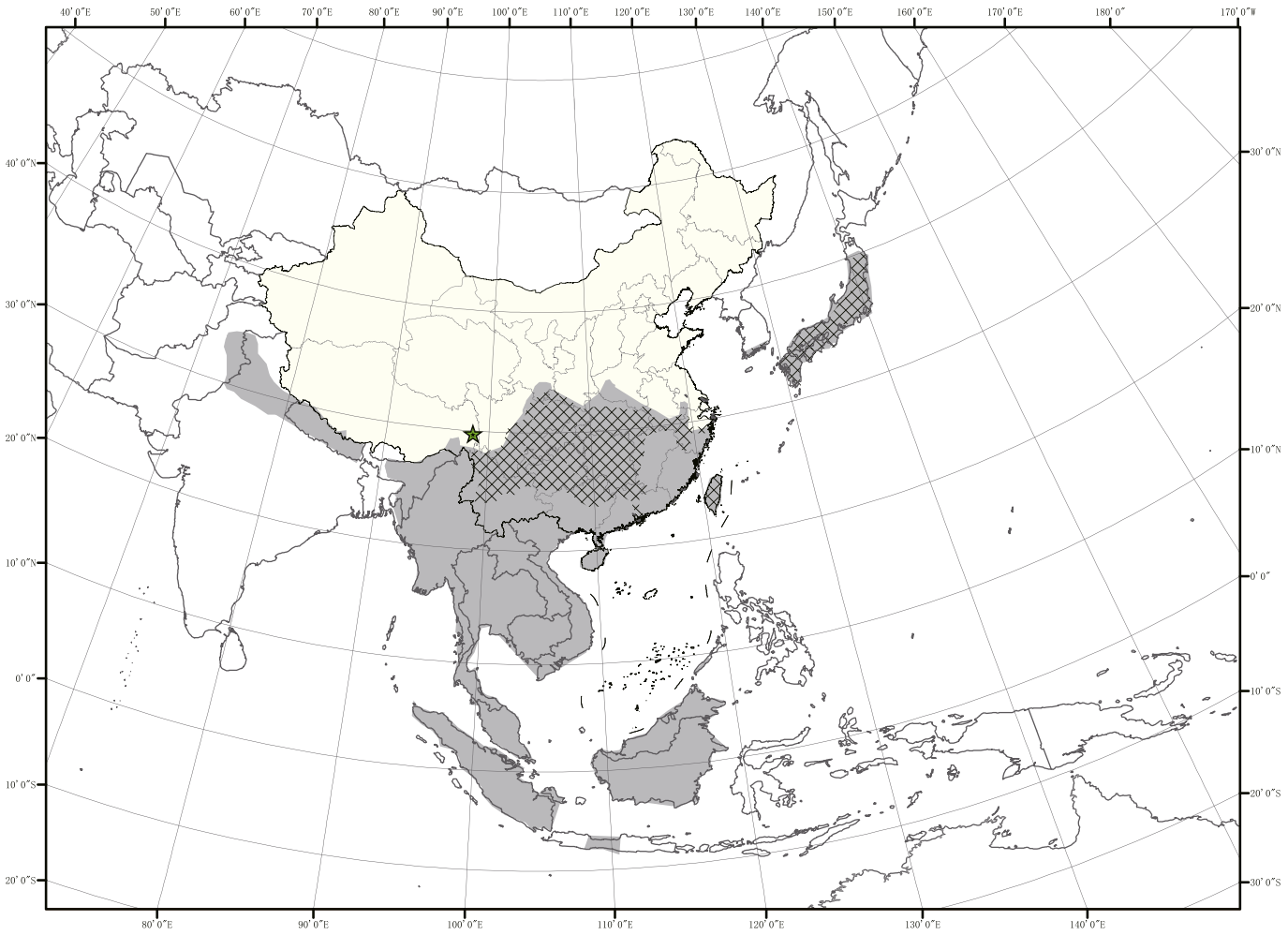

Fig. 1. Fossil locality in this study (a star), the distribution zone of *Quercus* subgenus *Cyclobalanopsis* (gray area), and distribution of nearest living relatives (NLRs) of *Quercus tibetensis* H. Xu, T. Su et Z.K. Zhou sp. nov. (gridded area). (For interpretation of the references to color in this figure legend, the reader is referred to the web version of this article.)

Tao and Du (1987) reported that the Lawula Formation flora is dominated by Betulaceae and they assigned the geological age to the late Miocene. We collected plant fossils from a layer of the Lawula Formation in the Kajun village (Kajun flora) where Fagaceae are the most abundant family, followed by Betulaceae (personal observations), and where *Elaeagnus tibetensis* T. Su et Z.K. Zhou (Elaeagnaceae) was recently reported (Su et al., 2014). Also, *Equisetum oppositum* H.J. Ma, T. Su et S.T. Zhang (Equisetaceae) has been found in the upper layer of the same strata (Ma et al., 2012). This vegetation association is similar to the late Miocene floras in Yunnan Province, a region adjacent to Mangkang County, e.g., the Xiaolongtan flora (Zhou, 1985), the Bangmai flora (Tao and Chen, 1983; Guo, 2011), and the Xianfeng flora (Xing, 2010). In this study, we assign the geological age of the Lawula Formation and the Kajun flora contained within to the late Miocene based on floristic comparison, regional geological structure, and stratigraphic correlations as proposed by previous studies (Tao and Du, 1987; Bureau of Geology and Mineral Resources of Xizang, 1993).

2.2. Leaf fossil morphology

We selected leaf fossils with morphological characteristics typical of the Fagaceae for our study. These include fossil leaves with straight midveins, straight parallel secondary veins, and a simple single serrate tooth per secondary vein (Jones, 1986; Tanai, 1995). Selected specimens were photographed with a Nikon D700 digital camera. When necessary, specimens were immersed in aviation kerosene to improve the contrast. Then, detailed morphological characters were examined and photographed with a stereomicroscope (Zeiss SteREO Discovery V20). All fossil materials in this study were preserved as impressions so we could not observe any cuticle.

To determine the taxonomic affinity of the fossil specimens, we compared them with vouchers of modern Fagaceae species housed at the Kunming Institute of Botany (KUN), and Xishuangbanna Tropical Botanical Garden (HITBC) herbaria, and electronic photos of specimens in the Herbarium of the French National Museum of Natural History (http://www.mnhn.fr), Herbarium of Royal Botanical Gardens, Kew (http://www.kew.org/), and the Chinese Virtual Herbarium (CVH; http://www.cvh.org.cn). Also, we prepared cleared leaves of extant species following the method of Foster (1952). Specimens of the cleared modern leaves are housed at the laboratory of the Paleoecology Research Group, Xishuangbanna Tropical Botanical Garden, Chinese Academy of Sciences. The terminology used to describe leaf morphology follows the Leaf Architecture Working Group (Ellis et al., 2009).

Hierarchical clustering was used to determine leaf morphology similarity among the newly discovered fossils and modern species in *Quercus* subgenus *Cyclobalanopsis*. We selected 27 modern species for further comparison based on the gross leaf morphology (Appendixes A and B). These modern species share several characters with our leaf fossils: (1) elliptic to narrow elliptic laminar shape, (2) microphyll laminar size, (3) laminar margin teeth distributed along the apical half to three fourths of the leaf, (4) symmetrical laminar shape, and (5) straight or uniformly curved secondary veins. A data matrix was built based on 17 leaf characters (Table 1) for each species. The primary data matrix was analyzed using complete hierarchical clustering in R (version 2.11.1; R Development Core Team, Vienna, Austria). Detailed information on hierarchical clustering of the 27 modern species and our leaf fossils is listed in Appendix A.

2.3. Distribution and climatic tolerance of living species in *Quercus* subgenus *Cyclobalanopsis*

We accessed occurrence data for about 400 specimens of modern species in *Quercus* subgenus *Cyclobalanopsis* to get detailed information on their distributions (longitude, latitude, and elevation) from the Chinese Virtual Herbarium (CVH; http://www.cvh.org.cn), the Tokyo National Museum of Nature and Science natural history collection database (http://www.science-net.kahaku.go.jp/), Flora of Pakistan (http://www.tropicos.org), the botany collection database of the London Natural History Museum (http://www.nhm.ac.uk), and the National Herbarium of The Netherlands (NHN) online (http://vstbol.leidenuniv.nl/) (Fig. 1). We calibrated the primary specimen data in Google Earth. Data for six climate parameters were recorded for each of the 400 specimen records using a global gridded climate dataset (http://www.worldclim.org/) with 30 arc-seconds resolution (Hijmans et al., 2005). These include: mean annual temperature (MAT), temperature annual range (TAR), mean temperature of warmest quarter (MTWQ), mean temperature of coldest quarter (MTCQ), mean annual precipitation (MAP), precipitation of warmest quarter (PWQ), and precipitation of coldest quarter (PCQ).

Table 1
Leaf characters and character states used in hierarchical clustering.

No	Character	Character state
1	Laminar L:W ratio	Quantitative
2	Leaf shape index (W3 − W1) / W2	Quantitative
3	Leaf-margin tooth number (TN)	Quantitative
4	Major secondary vein numbers	Quantitative
5	Major secondary numbers per cm 50% of middle leaf	Quantitative
6.1	Laminar shape	Elliptic
6.2		Ovate
6.3		Obovate
7.1	Base symmetry	Symmetrical
7.2		Asymmetrical
7.3		Basal insertion asymmetrical
8.1	Tooth type (distal flank come first)	Concave straight
8.2		Concave–concave
9.1	Tooth shape	Acute triangular
9.2		Sharp obtuse triangular
9.3		Rough obtuse triangular
10.1	Laminar margin tooth part percentage type	Untoothed or less tooth around the apex
10.2		Less than half of the margin toothed
10.3		More than one third of the margin toothed
10.4		More than half to one third of the margin toothed
11.1	Laminar apex shape	Straight
11.2		Acuminate
11.3		Straight to acuminate
12	Laminar base angle	Obtuse
13.1	Laminar base shape	Straight cuneate
13.2		Convex rounded
14.1	Major secondary veins course	Straight
14.2		Straight and curve near the margin
14.3		Curve near midvein straight near margin
15.1	Major secondary veins attachment to midvein	Decurrent
15.2		Excurrent

2.4. Paleoelevation estimate of the fossil site

We used the altitudinal distribution ranges of the nearest living relatives (NLRs) of *Q. tibetensis* to estimate paleoelevation of the fossil site during the late Miocene. In this procedure, the global paleoclimate background was considered, and the lapse rate of temperature along altitudes was used to calibrate the paleoaltitude (Sun et al., 2015). Then, the uplift of the fossil site was calculated as the difference of altitudes between the late Miocene and the present day.

$$H_{\text{fossil}} = H_{\text{NLR}_S} + \frac{MAT'_{\text{Miocene}}}{LAPSE_{\text{Miocene}}} \quad (1)$$

(Sun et al., 2015).

H_{fossil} (m) is the estimated paleoelevation of the late Miocene for the fossil site; H_{NLRs} is the upper and lower elevation limits of the NLRs, we

used 70 m to 3000 m (Table 3) here; $MAT'_{Miocene}$ is the difference of global mean annual temperature (MAT) between the late Miocene and the present, we used 4.50 °C by following Pound et al. (2011); $LAPSE_{Miocene}$ is the temperature lapse rate along altitudes during the Miocene, we used a lapse rate of −6.01 °C/1000 m (Song et al., 2010).

3. Results

3.1. Systematics

Order: Fagales Engler
Family: Fagaceae Dumortier
Genus: *Quercus* L.
Subgenus: *Cyclobalanopsis* (Oersted) Schneider
Species: *Quercus tibetensis* H. Xu, T. Su et Z.K. Zhou sp. nov.
Holotype: KUN PC2015009 (Plate I, A) (designated here).
Paratypes: KUN PC2015010 (Plate I, B), KUN PC2015011 (Plate I, C), KUN PC2015012 (Plate I, D), KUN PC2015013 (Plate I, E) KUN PC2014014 (Plate I, F) (designated here).
Repository: Herbarium of Kunming Institute of Botany, Chinese Academy of Sciences (KUN).
Type locality: The late Miocene Lawula Formation, Kajun village, Mangkang County, eastern Tibet, China.
Etymology: The specific epithet, *tibetensis*, refers to where these fossils were collected.
Diagnosis: Leaves elliptic, symmetrical, apex acuminate, base cuneate or rounded. Simple tooth concave–concave (CC–CC) or concave–straight (CC–ST) separated by rounded sinus. Straight or uniformly curved secondary veins excurrent near midvein. Tertiary veins opposite percurrent.
Description: Leaf is simple (Plate I, B), symmetrical (Plate I, D, E) to less commonly asymmetrical (Plate I, A, C), and the shape is elliptic (Plate I, C), or obovate (Plate I, A, E). Microphyll laminar is 3.4–7.5 cm long and 1.2–3.2 cm wide. Laminar length to maximal width ratio (L:W) is ca. 2.0–3.9. Leaf apex is acuminate; leaf base is cuneate or rounded. Leaf petiole is 0.5–0.8 cm long, 0.1–0.2 cm wide. Laminar margin teeth are acute, regularly spaced, developing on the apical half or two-thirds of the laminar margin (Plate I, B–E). CC–CC (Plate I, C–E) or CC–ST teeth (Plate I, A), with concave distal flank and concave or straight proximal flank, typically separated by rounded sinus (Plate I, A, C–E). Midvein is straight (Plate I, A–E). Secondary veins are straight or uniformly curved and are non-typical semicraspedodromous (Hickey, 1973; Leng, 1999) (Plate I, F–H). Secondary veins in the serrate part of the leaf branch into two veins when reaching the laminar margin; the stronger vein arrives at the tooth; the weaker vein deflects upward and joins the adjacent secondary vein (Plate I, H). Secondary veins in the lower part of the leaf are eucamptodromous so that secondary veins connect to superjacent secondary veins via tertiary veins, without forming marginal loops (Plate I, A). Nine to 13 pairs of secondary veins are regularly spaced within a leaf blade (Plate I, A–E). The angle of origin of the secondary veins to the midvein is constant or increases proximally ca. 35–80°. Intersecondary veins are present (Plate I, E). Percurrent tertiary veins are opposite so that the tertiary veins cross between adjacent secondary veins in parallel paths without branching (Plate I, F). The angle of the tertiary vein to the secondary vein is RR (Plate I, A, C) so that tertiary veins form a right angle (R) with the admedial side of the secondary veins, and a right angle (R) with the exmedial side of the secondary

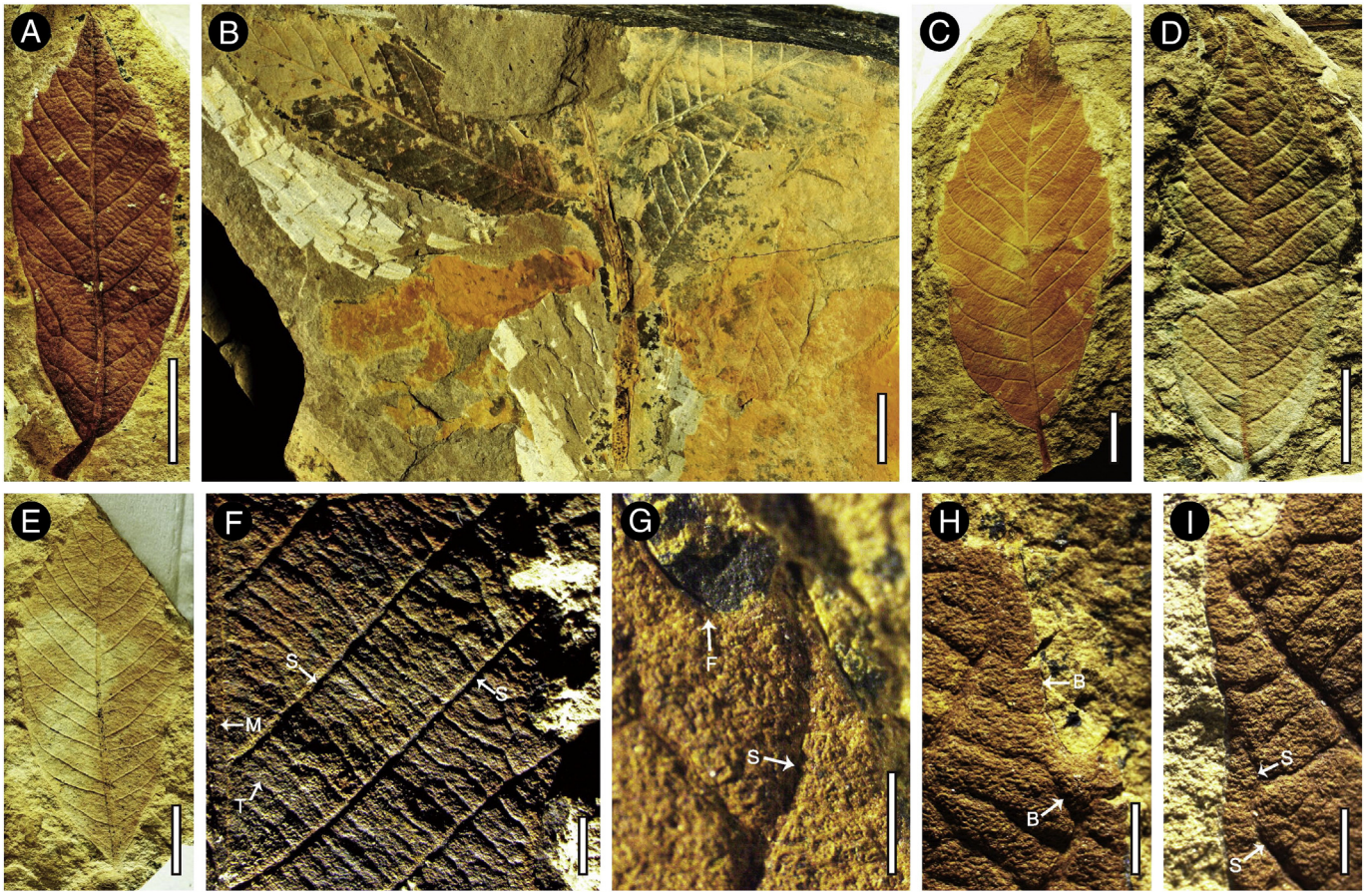

Plate I. *Quercus tibetensis* H. Xu, T. Su et Z.K. Zhou sp. nov. from the late Miocene of Tibet, China. Leaves and a branch (A–E): KUN PC2015009 (A), 2015010 (B), 2015011 (C), 2015012 (D), and 2015013 (E), scale bars = 1 cm. Straight secondary veins (F–I): KUN PC2015014 (F), scale bar = 2 cm; 2015009 (G–I), scale bars = 1 cm. B = branched secondary veins; F = fimbrial vein; M = midvein; S = secondary vein; T = tertiary vein.

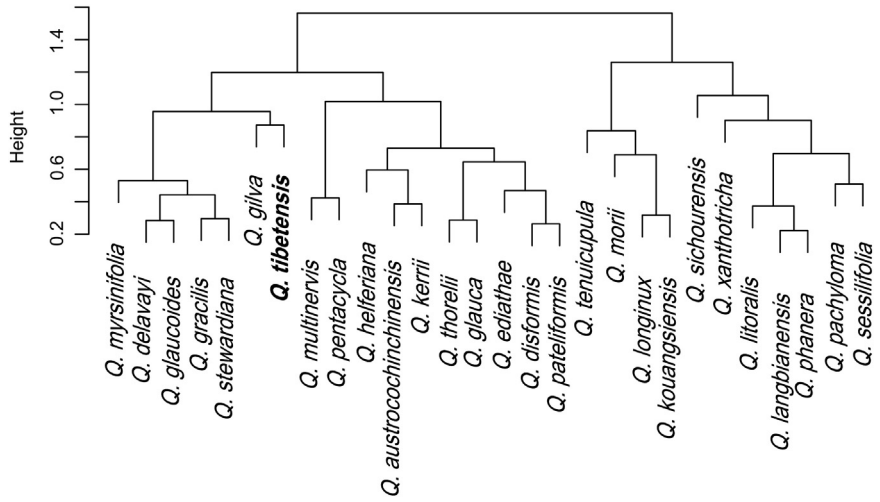

Fig. 2. The cluster result showing the morphological similarity among *Quercus tibetensis* H. Xu, T. Su et Z.K. Zhou sp. nov. and 27 extent species of *Quercus* subgenus *Cyclobalanopsis*. See also Appendix A for character matrix.

veins. The angle of the percurrent tertiary vein to the midvein increases towards the base (Plate I, A, C).

3.2. Nearest living relatives of Q. tibetensis

The hierarchical clustering results indicated that six living species of ring-cupped oaks, *Quercus delavayi* Franch., *Quercus gilva* Blume, *Quercus glaucoides* M. Martens & Galeotti, *Quercus gracilis* Korth., *Quercus myrsinifolia* Blume, and *Quercus stewardiana* A. Camus, were the most similar to our leaf fossils in terms of their morphology, so we considered them the nearest living relatives (NLRs) of *Q. tibetensis* (Fig. 2). Based on limited morphological features of *Q. tibetensis* due to the preservation condition, it was hard to conclude which specific species showed the closest morphological similarity to *Q. tibetensis*.

3.3. Climatic tolerance of extant ring-cupped oaks

Today, ring-cupped oaks live in regions with mean annual temperature values (MAT) between 7.4 °C and 23.8 °C and mean annual precipitation values (MAP) ranging from 627.0 mm to 2536.8 mm (Table 2). The nearest living relatives (NLRs) of *Q. tibetensis* as determined through our cluster analysis, are distributed in areas with MAT values between 7.9 °C (*Q. gracilis*) and 21.7 °C (*Q. myrsinifolia*), and MAP values between 733.0 mm (*Q. gracilis*) and 2536.8 mm (*Q. gilva*) (Table 2, Fig. 3).

3.4. Paleoelevation estimation

To estimate the paleoevelation of the Kajun flora, we calculated the minimum and maximum elevation limits of the Nearest Living Relatives (NLRs) of *Q. tibetensis* assuming that Miocene global temperatures were on average 4.5 °C warmer than today (Pound et al., 2011). The NLRs of *Q. tibetensis* have upper elevation limits of 2070 to 3000 m, with lower elevation limits of 70 to 800 m (Table 3). Among these NLRs, *Q. glaucoides* is found in locations up to 3000 m in elevation (Table 3, Fig. 4). Using Eq. (1), we calculated that *Q. glaucoides* could grow as high as 3749 m given warmer Miocene conditions. Therefore, we suggest that the paleoelevation of the Kajun flora ranged between 819 and 3749 m. The difference between these elevation estimates and the modern elevation of the fossil site (3910 m) suggests that the Kajun flora grew between 161 and 3091 m lower than where the site is positioned today.

4. Discussion

4.1. Systematic assignment of the leaf fossils

Our leaf fossils are assigned to Fagaceae based on gross characters, e.g., equally spaced secondary veins and a single serrate tooth per secondary vein along the laminar margin (Jones, 1986; Tanai, 1995; Luo and Zhou, 2002). Some characters, namely, the presence of straight midvein (Plate I, A–E; Plate II, A, B, C), simple tooth per secondary vein (Plate I, A–E; Plate II, A, B, C), semicraspedodromous secondary veins (Plate I, F–H; Plate II, A, B, C, D), and fimbrial veins (Plate I, G; Plate II, D, E, F), indicate that our leaf fossils resemble the serrate leaves of *Castanopsis* (D. Don) Spach, *Lithocarpus* Blume and *Quercus* L. (Table 4).

The serrate leaves of *Castanopsis* usually possess zigzag secondary veins when they reach the laminar margin (Plate II, G; Table 4). There are some exceptions, whose secondary veins are straight or uniformly

Table 2
Climate data from a global gridded climate dataset (http://www.worldclim.org/) within the distribution of nearest living relatives (NLRs) of *Quercus tibetensis* H. Xu, T. Su et Z.K. Zhou sp. nov., including: *Q. delavayi* Franch., *Q. gilva* Blume, *Q. glaucoides* M. Martens & Galeotti, *Q. gracilis* Korth., *Q. myrsinifolia* Blume, and *Q. stewardiana* A. Camus.

	MAT (°C)	MTWQ (°C)	MTCQ (°C)	TAR (°C)	MAP (mm)	PWQ (mm)	PCQ (mm)
Quercus subgenus *Cyclobalanopsis*	7.4–23.8	10.8–31.7	(−2)–17.2	8.8–36.7	627–2536.8	304.4–1664.3	12–555.8
NLRs of *Quercus tibetensis*	7.9–21.7	14.1–28.4	(−2)–15.3	18.1–34.3	733–2536.8	403.3–1157.5	12–454.8
Quercus delavayi	10.8–16.7	16.5–25.3	4.2–9.6	22.5–28.2	892.5–1203.6	472.2–650.8	14–68.2
Quercus gilva	13.7–17.9	23.6–28.4	4.2–8.7	26.6–33.1	1328.3–2536.8	435–939.8	107.5–454.8
Quercus glaucoides	9–18.9	14.1–25.4	2.4–12	22.4–27.8	794.3–1333	417.5–716	12–62.8
Quercus gracilis	7.9–18.5	16.4–27.2	(−1.9)–9.7	25.4–33.6	733–1980	410–732.8	13–234
Quercus myrsinifolia	9.4–21.7	20.7–27.1	(−2)–15.3	18.1–34.3	814–2247.3	403.3–1157.5	19–230.3
Quercus stewardiana	7.9–17.5	15.8–26.5	(−1.3)–7.8	22.2–30.5	1272.3–1960.3	534.3–744.8	48.3–224.5
Kajun, Mangkang	4.4	11.5	−3.25	29.3	516.5	312.5	9.5

MAT: mean annual temperature; TAR: temperature annual range, MTWQ: mean temperature of warmest quarter, MTCQ: mean temperature of coldest quarter, MAP: mean annual precipitation, PWQ: precipitation of warmest quarter, PCQ: precipitation of coldest quarter.

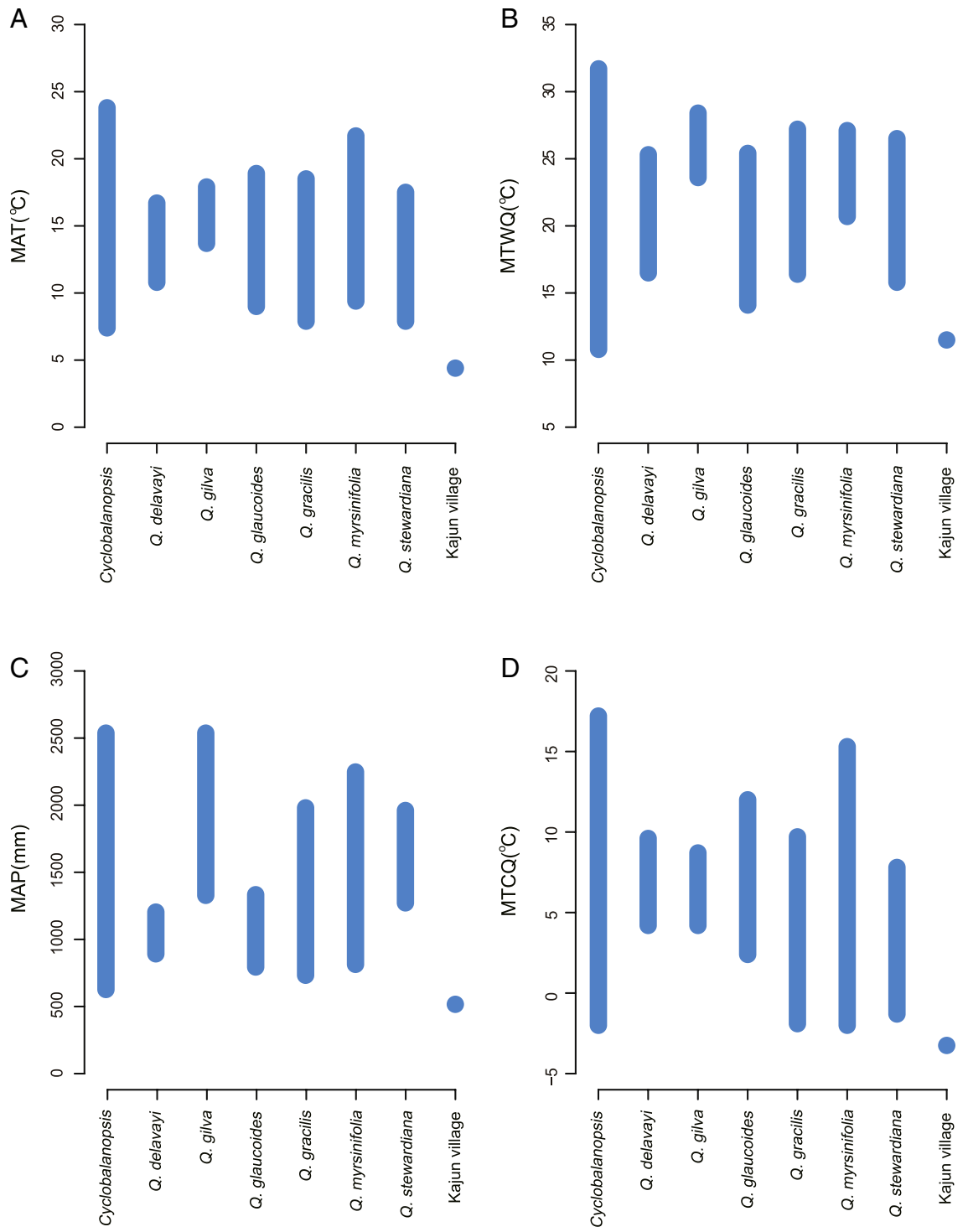

Fig. 3. Climate niche of *Quercus* subgenus *Cyclobalanopsis* and nearest living relatives (NLRs) of *Quercus tibetensis* H. Xu, T. Su et Z.K. Zhou sp. nov., namely *Q. delavayi* Franch., *Q. gilva* Blume, *Q. glaucoides* M. Martens & Galeotti, *Q. gracilis* Korth., *Q. myrsinifolia* Blume, and *Q. stewardiana* A. Camus. MAT = mean annual temperature, TAR = temperature annual range, MTWQ = mean temperature of warmest quarter, MTCQ = mean temperature of coldest quarter, MAP = mean annual precipitation, PWQ = precipitation of warmest quarter, and PCQ = precipitation of coldest quarter.

curved, e.g., *Castanopsis cerebriana* (Hickel & A. Camus) Barnett, *Castanopsis choboensis* Hickel & A. Camus, *Castanopsis clarkei* King ex Hook. f., *Castanopsis fissa* (Champ. ex Benth.) Rehder & E.H. Wilson, and *Castanopsis indica* (J. Roxb. ex Lindl.) A. DC. However, a few features, for instance, an oblique laminar base (*C. choboensis*, *C. clarkei*, *C. indica*), and more than 20 pairs of secondary veins (*C. cerebriana*, *C. fissa*), are markedly different from our leaf fossils.

Many *Lithocarpus* species have entire leaves (Jones, 1986), while a few species with serrate leaves are found in China, e.g., *Lithocarpus carolineae* (Skan) Rehder, *Lithocarpus corneus* (Lour.) Rehder, *Lithocarpus konishii* (Hayata) Hayata, and *Lithocarpus pachyleipis* A. Camus (Huang et al., 1999). Characters such as a bullate leaf (*L. corneus*), more than 15 secondary veins (*L. corneus*, *L. pachyleipis*), secondary veins abruptly curving apically near margin (*L. carolineae*, *L. corneus*)

Table 3
Elevation ranges of nearest living relatives (NLRs) of *Quercus tibetensis* H. Xu, T. Su et Z.K. Zhou sp. nov.

Species	Altitude range (m)	Location of altitude limit	Specimen number	Estimate paleoaltitude (m)	Estimate paleoaltitude change (m)
Q. delavayi	720–2750	Fuling County, Sichuan China	CDBI0013603	1469	2441
		Dayao County, Yunnan China	KUN0670133	3499	411
Q. gilva	200–2070	Nanyue County, Hunan China	PE00310169	949	2961
		Hezhang County, Guizhou China	IBSC0042074	2819	1091
Q. glaucoides	680–3000	Cangyuan County, Yunnan China	KUN0500639	1429	2481
		Songming County, Yunnan China	PE00311514	3749	161
Q. gracilis	70–2600	Jiande County, Zhejiang China	PE00311651	819	3091
		Nanchuan County, Sichuan China	PE00311868	3349	561
Q. myrsinifolia	700–2500	Xiushui County, Jiangxi China	KUN0506444	1449	2461
		Gongshan County, Yunnan China	KUN0455110	3249	661
Q. stewardiana	800–2800	Longquan County, Zhejiang, China	PE00310359	1549	2361
		Fanjingshan, Guizhou China	PE00381461	3549	361
NLRs	70–3000				161
					3091

PE: Chinese National Herbarium; CDBI: herbarium of Chengdu Institute of Biology, Chinese Academy of Sciences; KUN: herbarium of Kunming Institute of Botany, Chinese Academy of Sciences; IBSC: herbarium of South China Botanical Garden, Chinese Academy of Sciences.

(Plate II, D, H; Huang et al., 1999), and obtuse teeth (*L. konishii*), indicate that our leaf fossils do not closely match the serrate leaves in *Lithocarpus*.

Some species in *Quercus* subgenus *Quercus* possess straight midveins and serrated margins along the apical two thirds to half of the leaves, which is similar to our fossils. However, several traits of *Quercus* subgenus *Quercus* species differ from our leaf fossils, e.g., spinose teeth (subsection *Campylolepides*, *Quercus engleriana* Seemen, *Quercus setulosa* Hickel & A. Camus, *Quercus tarokoensis* Hayata), modified urticoid tooth type I (subsection *Diversipilosae*, Leng, 1999), in that the medial vein terminates beyond the tooth apex and forms a very short mucro (Hickey and Wolfe, 1975), zigzag secondary veins at the laminar margin (*Quercus franchetii* Skan, *Quercus lanata* Sm., *Quercus lanuginosa* Beck, *Quercus leucotrichophora* A. Camus, *Quercus lodicosa* O.E. Warb. & E.F. Warb.), and a truncate laminar base (*Quercus oxyphylla* (E.H. Wilson) Hand.-Mazz.). Among subgenus *Quercus*, *Q. engleriana*, and *Q. lanata* within section Engleriana, possess many leaf characters that are similar to those in our fossils. Several characters of *Q. engleriana*, such as, a straight secondary vein and some secondary veins branching at the midpoint and terminating at the teeth, are similar to the venation in our fossils. But *Q. engleriana* differs from our leaf fossils in possessing spinose teeth. Therefore, we exclude the possibility of the assignment of our fossils to the subgenus *Quercus*.

Our leaf fossils share many characteristics with species in *Quercus* subgenus *Cyclobalanopsis*, such as a symmetrical laminar shape (Plate I, D–E; Plate II, A) and straight or uniformly curved secondary veins that are equally spaced (Plate I, A–E; Plate II, A; Table 4).

Fossil records of *Quercus* subgenus *Cyclobalanopsis* have been reported from Cenozoic strata ranging from Eocene to late Pliocene and are within the modern distribution scope of ring-cupped oaks (Colani, 1920; Kanehara, 1936; Tanai, 1953; Huzioka, 1963; Huzioka and Takahasi, 1970; Ishida, 1970; Guo, 1978; Writing Group of Cenozoic Plants of China, 1978; Zhang, 1978; Li and Guo, 1982; Tao and Chen, 1983; Zhou, 1993; Tanai, 1995; Zhou, 1996, 2000; Cheng, 2004; Yun, 2007; Jia et al., 2009; Wu, 2009; Khan et al., 2011). *Quercus* aff. *delavayi* (Jia et al., 2009) and *Quercus praegilva* (Zhou, 2000) differ from our leaf fossils in that they have a larger laminar length to maximal width ratio (Appendix B). *Quercus* cf. *patelliformis* (Wen, 2011), *Quercus praedelavayi* (Xing et al., 2013), *Quercus praegilva* (Zhou, 2000) and *Quercus tenuipilosa* (Hu et al., 2014) have decurrent secondary veins near the midvein (Appendix B), while secondary veins in our leaf fossils are excurrent near the midvein (Plate I, A–E). *Quercus ezoana* possesses small, sharp teeth that are not found in our leaf fossils (Tanai, 1995). Herein, we describe these fossils as a new species, *Q. tibetensis* H. Xu, T. Su et Z.K. Zhou sp. nov.

4.2. Southeastern Qinghai–Tibetan Plateau in the late Miocene had a warmer and wetter climate

Q. tibetensis is the first fossil record of *Quercus* subgenus *Cyclobalanopsis* in Tibet, which indicates that ring-cupped oaks existed during the late Miocene in the core area of the Qinghai–Tibetan Plateau. Leaves of *Q. tibetensis* are abundant in the Kajun flora, which may indicate an evergreen habitat, similar to all modern species of ring-cupped oaks. Meanwhile, some deciduous taxa, such as *Alnus*, *Betula* and *Populus* also occur in the Kajun flora. Therefore, the Kajun flora can be described as an evergreen–deciduous broadleaf forest. There are currently several vegetation types near the fossil site in Mangkang County, including deciduous broadleaf forest, mixed conifer-broadleaf forest, evergreen sclerophyllous broadleaf forest, conifer forest, and alpine meadow (Zhang et al., 1988; personal observation). Evergreen–deciduous broadleaf forests are found in warmer and more humid climates than the current climate near the fossil site (Zhang et al., 1988).

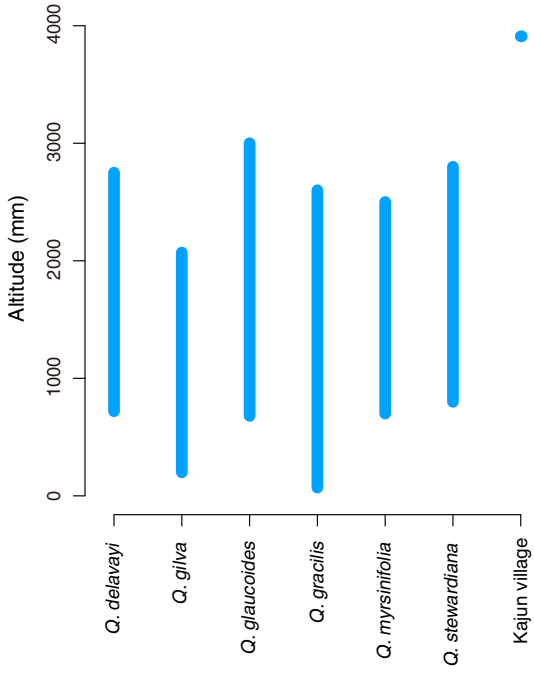

Fig. 4. Modern elevation of Kajun village and elevation ranges of the nearest living relatives (NLRs) of *Quercus tibetensis* H. Xu, T. Su et Z.K. Zhou sp. nov.

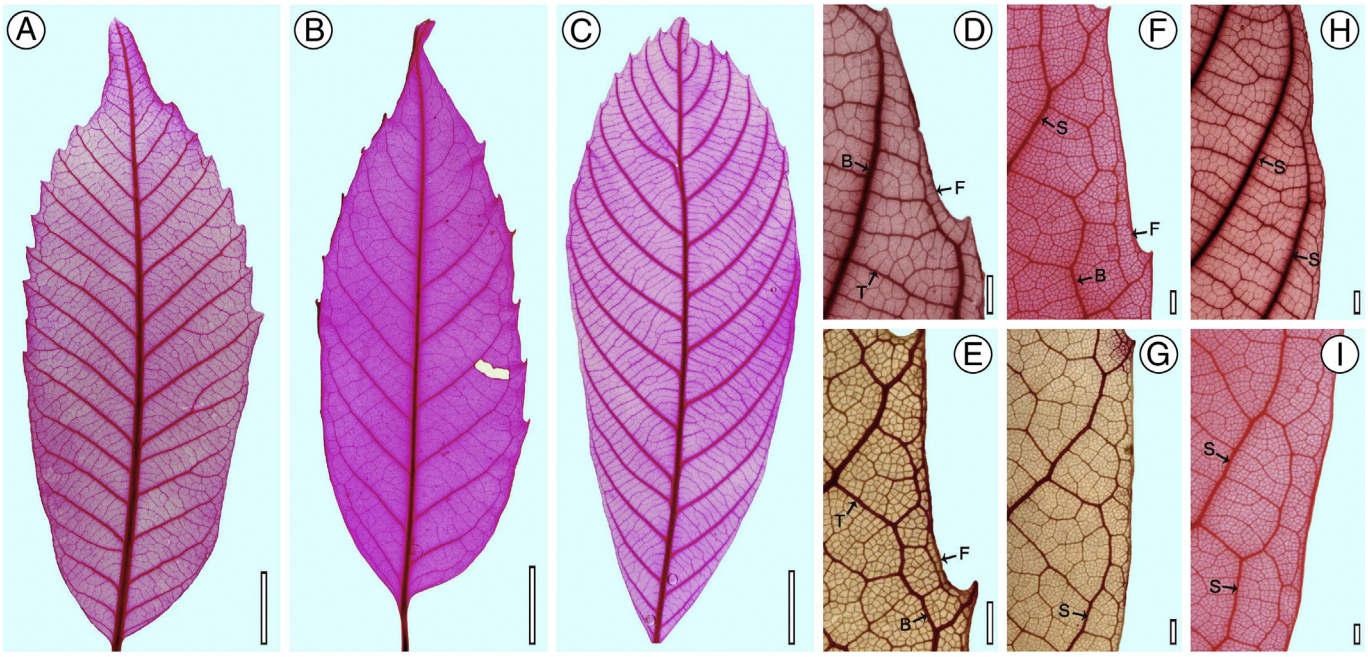

Plate II. Morphological comparison of leaf structure of *Quercus* subgenus *Cyclobalanopsis*, *Lithocarpus* and *Castanopsis*. A, E, G: *Quercus delavayi*; B, F, I: *Castanopsis chinensis*; C, D, H: *Lithocarpus carolineae*. B = branched secondary vein; F = fimbrial vein; S = secondary vein; T = tertiary vein. Scale bars = 1 cm.

Ring-cupped oaks are good indicators of paleoclimate conditions based on their tropical and subtropical distribution (Fig. 1; Soepadmo, 1972; Huang et al., 1999; Luo and Zhou, 2001) and extant species of ring-cupped oaks cannot persist in the current climate conditions where the fossils of *Q. tibetensis* were found. Most species of ring-cupped oaks live in forests in tropical or subtropical climates, while a few species live in a temperate climate, and are distributed in deciduous and evergreen broad-leaf forests and deciduous broadleaf mixed forests, near the northern border of the subtropical zone in China (Huang et al., 1999; Fig. 1), e.g., *Quercus glauca*, *Q. gracilis*, *Q. myrsinifolia*, and *Q. stewardiana* (Luo and Zhou, 2001). We used climate requirements of nearest living relatives (NLRs) of *Q. tibetensis* to explore its paleoclimate implications. The current mean annual temperature (MAT) of the fossil site is 4.4 °C, which is 3.5 °C lower than the minimum MAT requirement of NLRs (Table 2). Moreover, the lower limit of mean annual precipitation (MAP) among NLRs is slightly higher than that of the fossil site (Table 2). Therefore, the climate conditions in southeastern Qinghai–Tibetan Plateau during the late Miocene were likely warmer and more humid than they are today. Several methods could be applied to quantitatively reconstruct paleoclimate with the Kajun Flora in the future, such as Leaf Margin Analysis, Climate–Leaf Multivariate Analysis Program, and Coexistence Approach.

The climate conditions deduced from NLRs of *Q. tibetensis* are consistent with previous studies on paleoclimate in southwestern China. Paleoclimatic reconstructions for Yunnan, a province adjacent to eastern Tibet have been extensively studied using leaf physiognomy methods and the coexistence approach. These studies concluded that the climate was 1.2 °C to 3 °C warmer in MAT and 34.3 mm to 394.5 mm wetter in

Table 4
Morphological comparison among different genera in Fagaceae.
Data are from Hickey and Wolfe (1975), Zhou et al. (1995), Leng (1999), Luo (2000), and Liu (2010).

Taxa	Tooth type	Tooth number per secondary vein	Laminar symmetry	Laminar base	Midvein type	Venation type	Secondary vein course	Fimbrial vein
Fagus	Fagoid[a]	Entire or one	Symmetrical	Acute, cuneate, or rounded	Straight or sinuous to zigzag	Craspedodromous or semicraspedodromous	Straight or sinuous	Absent
Quercus subgenus *Quercus*	Glandular, spinose, modified urticoid I[b] or simple	One or two	Symmetrical	Acute, obtuse, cordate, auriculate, or rounded	Zigzag or straight	Craspedodromous or semicraspedodromous	Zigzag or straight	Present
Quercus subgenus *Cyclobalanopsis*	Simple tooth	One occasionally two	Symmetrical	Cuneate or wide cuneate	Straight	Semicraspedodromous, eucamptodromous or weak brochidodromous	Straight occasionally zigzag	Present
Castanea	Modified urticoid III (U3)[c]	One occasionally two	Symmetrical	Rounded, broadly cuneate, or truncate	Straight	Craspedodromous	Straight	Absent
Castanopsis	Simple tooth	One occasionally two	Symmetrical or asymmetrical	Cuneate, rounded, or convex	Straight or curve a little	Semicraspedodromous or festoonted eucamptodromous	Zigzag occasionally straight	Present
Lithocarpus	Entire, obtuse, or simple	Entire or one	Symmetrical	Cuneate, or cuneate to sharp	Straight or curve a little	Craspedodromous or semicraspedodromous	Straight	Present

[a] Fagoid: tooth is asymmetrical and has a medial vein surround by higher order veins. The medial vein rarely reaches laminar margin. The admedial vein is distinct and almost the same size with the medial vein (Leng, 1999).
[b] Modified urticoid I: medial vein terminates beyond the tooth apex, forming a very short mucro. Mucro generally inclines to leaf apex (Leng, 1999).
[c] Modified urticoid III (U3): tooth apex elongate but thin, sometimes the tooth apex is sickleform and inclines to the leaf apex. Tooth apex is made of veins and other leaf tissue (Leng, 1999).

MAP during the late Miocene than in the present day (Xia et al., 2009; Jacques et al., 2011; Xing et al., 2012). Furthermore, the climate conditions during the late Miocene in southeastern Qinghai–Tibetan Plateau are also in agreement with warmer Miocene global climate conditions calculated by climate models (Dutton and Barron, 1997; Micheels et al., 2007; Knorr et al., 2011; Yao et al., 2011) and oxygen isotope data (Zachos et al., 2008). The continued uplift of the Qinghai–Tibetan Plateau and global cooling and drying since the Miocene (Miao et al., 2012) may have contributed to the cooler and drier climate currently found in southeastern Qinghai–Tibetan Plateau.

4.3. Continued uplift of the Qinghai–Tibetan Plateau since the late Miocene

There is significant elevation difference between the fossil site and modern distributions of *Cyclobalanopsis* (Table 3). Today, none of the extant ring-cupped oaks could survive at elevations of approximately 4000 m in Mangkang County, near the fossil site. The maximum elevation limit of most extant ring-cupped oaks is 2000 m or less (Luo and Zhou, 2001); though a few species do survive at higher altitudes, e.g., *Quercus steenisii* with 3460 m in Indonesia. In southwest China, some species of ring-cupped oaks survive at elevations ranging from 2000 m to 3000 m (Luo and Zhou, 2001; Wu, 2008).

Plant distributions change as the climate (Woodward, 1987) and elevation changes (Hooghiemstra et al., 2006); therefore, the paleoclimate condition should be taken into account when considering the distribution and elevation of plants over geological time. In this study, six living species show close affinity to *Q. tibetensis* based on detailed comparison of leaf morphology, namely, the Nearest Living Relatives (NLRs). Their altitude distribution ranges are much lower than the present altitude of the fossil site (Table 3). A warmer climate than the present day occurred during the late Miocene, and we estimated the paleoelevation of the site by determining the maximum elevations that the NLRs of *Q. tibetensis* could survive given a higher global mean annual temperature of 4.5 °C (Pound et al., 2011). The results showed that the NLRs of *Q. tibetensis* could not withstand growing conditions at the present day elevation of the fossil site, even taking into account warmer climate during the Miocene (Table 3). Among NLRs of *Q. tibetensis*, *Q. glaucoides* distributes in the highest altitude, up to 3000 m in Yunnan, the estimated paleoelevation of the fossil site during the late Miocene was still at least 160 m lower than the modern elevation.

Therefore given the assumptions of our model, the occurrence of *Q. tibetensis* at a high elevation in eastern Tibet indicates the continued uplift of eastern Tibet since the late Miocene. Besides *Q. tibetensis*, the Kajun flora contains *Elaeagnus tibetensis* (Su et al., 2014) and *Alnus* at an elevation that is also beyond the maximum elevation of any modern species in those genera. Our results conform with other studies that suggest a continued rise of the southeastern Qinghai–Tibetan Plateau during the late Miocene. Clark et al. (2005) used thermochronologic data to estimate the erosion rate of southeastern Tibet, and they suggested high topography began to develop during the late Miocene. Another study that used similar methods indicated that Chayu County, close to Mangkang County, uplifted dramatically during the late Miocene (Lei et al., 2008). Additionally, Westaway (2009) used sedimentary and geomorphological data from the Yangtze and Red River systems in Yunnan, southeastern margin of the Qinghai–Tibetan Plateau, and suggested the uplift of about 3 km there since 8 Ma. A Pliocene uplift in this region was also suggested by using data from thermochronology, mapping, sedimentology, and paleobotany (Schoenbohm et al., 2006). Meanwhile, the uplift of the southeastern Qinghai–Tibetan Plateau is documented by the dramatic vegetation changes in the Neogene: the late Miocene Kajun flora is dominated by *Quercus* subgenus *Cyclobalanopsis*, whereas the late Pliocene floras nearby are rich in *Quercus* section *Heterobalanus* (Tao and Kong, 1973; Tao, 2000; Su, 2010), which usually occurs in subalpine or alpine regions of southwestern China. Hence, our data may help constrain the age of an additional pulse of uplift between the late Miocene and the late Pliocene. We interpret the occurrence of *Q. tibetensis* at a present day elevation of ~4 km, and the altitudinal difference of the fossil site of 161 m to 3091 m between the late Miocene and today as evidence for continued uplift of the southeastern Qinghai–Tibetan Plateau since the late Miocene. More work with other taxa as well as the whole assemblage of plants from the Kajun flora is needed to improve our understanding of paleoenvironmental change in southeastern Qinghai–Tibetan Plateau.

Supplementary data to this article can be found online at http://dx.doi.org/10.1016/j.palaeo.2015.11.014.

Acknowledgements

We thank members of the Paleoecology Research Group in Xishuangbanna Tropical Botanical Garden for fossil collection; J.J. Hu for providing leaves of modern species; Central Laboratory of Xishuangbanna Tropical Botanical Garden for technical support of images; and two reviewers for many constructive suggestions. This work is supported by the National Natural Science Foundation of China (31470325; U1502231), the 973 Project (No. 2012CB821900), the Foundation of the State Key Laboratory of Paleobiology and Stratigraphy, Nanjing Institute of Geology and Paleontology, CAS (No. 143107), as well as the CAS 135 program (XTBG-F01). This work is a contribution to NECLIME (Neogene Climate Evolution in Eurasia).

References

An, Z.S., Kutzbach, J.E., Prell, W.L., Porter, S.C., 2001. Evolution of Asian monsoons and phased uplift of the Himalaya–Tibetan plateau since Late Miocene times. Nature 411, 62–66.

Bureau of Geology and Mineral Resources of Xizang (BGMRX), 1993. Regional Geology of Yunnan Province. Geological Publishing House, Beijing (in Chinese with English summary).

Cheng, Y.M., 2004. Pliocene wood flora from Yuanmou of Yunnan and Taigu of Shanxi, China (Ph.D. Dissertation) Institute of Botany, Chinese Academy of Sciences (in Chinese with English abstract).

Clark, M.K., House, M.A., Royden, L.H., Whipple, K.X., Burchfiel, B.C., Zhang, X., Tang, W., 2005. Late Cenozoic uplift of southeastern Tibet. Geology 33 (6), 525–528.

Colani, M., 1920. Étude sur les flores tertiaires de quelques gisements de lignite de l' Indochine et du Yunnan. Bull. Serv. Géol. Indochine 8 (1), 1–524.

Ding, L., Xu, Q., Yue, Y.H., Wang, H.Q., Cai, F.L., Li, S., 2014. The Andean-type Gangdese Mountains: Paleoelevation record from the Paleocene–Eocene Linzhou Basin. Earth Planet. Sci. Lett. 392, 250–264.

Dutton, J.F., Barron, E.J., 1997. Miocene to present vegetation changes: a possible piece of the Cenozoic puzzle. Geology 25 (1), 39–41.

Ellis, B., Daly, D.C., Hickey, L.J., Johnson, K.R., Mitchell, J.D., Wilf, P., Wing, S.L., 2009. Manual of Leaf Architecture. Cornell University Press, New York.

England, P.C., Houseman, G.A., 1989. Extension during continental convergence, with application to the Tibetan Plateau. J. Geophys. Res. 94, 17561–17579.

Fang, A.M., Yan, Z., Liu, X.H., Pan, Y.S., Li, J.L., Yu, L.J., Huang, F.X., Tao, J.R., 2006. The age of the paleoflora in Liuqu conglomerates of Southern Tibet and its tectonic implications. Nat. Sci. Prog. 16 (1), 55–64.

Foster, A.S., 1952. Foliar venation in angiosperms from an ontogenetic standpoint. Am. J. Bot. 39, 752–766.

Guo, S.X., 1978. Pliocene floras of western Sichuan. Acta Palaeontol. Sin. 17, 343–352 (in Chinese with English abstract).

Guo, S.X., 2011. The late Miocene Bangmai flora from Lincang County of Yunnan, southwestern China. Acta Palaeontol. Sin. 50, 353–408 (in Chinese with English abstract).

Harrison, T.M., Yin, A., 2004. Timing and processes of Himalayan and Tibetan uplift. Himal. J. Sci. 2 (4), 152–153.

Hickey, L.J., 1973. Classification of the architecture of dicotyledonous leaves. Am. J. Bot. 60, 17–33.

Hickey, L.J., Wolfe, J.A., 1975. The bases of angiosperms phylogeny: vegetative morphology. Ann. Mo. Bot. Gard. 62, 538–589.

Hijmans, R.J., Cameron, S.E., Parra, J.L., Jones, P.G., Jarvis, A., 2005. Very high resolution interpolated climate surfaces for global land areas. Int. J. Climatol. 25, 1965–1978.

Hooghiemstra, H., Wijninga, V.M., Cleef, A.M., 2006. The paleobotanical record of Colombia: implications for biogeography and biodiversity. Ann. Mo. Bot. Gard. 93 (2), 297–325.

Hu, Q., Xing, Y.W., Hu, J.J., Huang, Y.J., Ma, H.J., Zhou, Z.K., 2014. Evolution of stomatal and trichome density of the *Quercus delavayi* complex since the late Miocene. Chin. Sci. Bull. 59, 310–319.

Huang, C.C., Chang, Y.T., Bartholomew, B., 1999. Fagaceae. In: Wu, C.Y., Raven, P.H. (Eds.), Flora of China. Science Press and Missouri Botanical Garden Press, Beijing, St. Louis.

Huzioka, K., 1963. The Utto flora of northern Honshu. In: The Collaborating Association to Commemorate the 80th Anniversary of the Geological Survey of Japan (Ed.)Tertiary Floras of Japan I. Miocene Floras. Geol. Surv., Japan, Tokyo, pp. 153–216.

Huzioka, K., Takahasi, E., 1970. The Eocene flora of the Ube coal-field, southwest Honshu, Japan. J. Min. Coll. Akita Univ. Ser. A Min. Geol. 4 (5), 1–88.
Ishida, S., 1970. The Noroshi flora of the Noto Peninsula, central Japan. Mem. Fac. Sci. Kyoto Univ. ser. Geol. Mineral 37 (1), 1–112.
Jacques, F.M.B., Guo, S.X., Su, T., Xing, Y.W., Huang, Y.J., Liu, Y.S.C., Ferguson, D.K., Zhou, Z.K., 2011. Quantitative reconstruction of the Late Miocene monsoon climates of southwest China: a case study of the Lincang flora from Yunnan Province. Palaeogeogr. Palaeoclimatol. Palaeoecol. 304, 318–327.
Jacques, F.M.B., Su, T., Spicer, R.A., Xing, Y.W., Huang, Y.J., Zhou, Z.K., 2014. Late Miocene southwestern Chinese floristic diversity shaped by the southeastern uplift of the Tibetan Plateau. Palaeogeogr. Palaeoclimatol. Palaeoecol. 411, 208–215.
Jia, H., Sun, B.N., Li, X.C., Xiao, L., Wu, J.Y., 2009. Microstructures of one species of *Quercus* from the Neogene in Eastern Zhejiang and its palaeoenvironmental indication. Earth Sci. Front. 16, 79–90 (in Chinese with English abstract).
Jones, J.H., 1986. Evolution of the Fagaceae: the implications of foliar features. Ann. Mo. Bot. Gard. 73 (2), 228–275.
Jordan, G.J., 2011. A critical framework for the assessment of biological palaeoproxies: predicting past climate and levels of atmospheric CO_2 from fossil leaves. New Phytol. 192, 29–44.
Kanehara, K., 1936. The geology of the northern part of Geizitu District, North Keisyodo, Korea. J. Geol. Soc. Jpn. 43, 73–103 (in Japanese).
Khan, M.A., Ghosh, R., Bera, S., Spicer, R.A., Spicer, T.E., 2011. Floral diversity during Plio-Pleistocene Siwalik sedimentation (Kimin Formation) in Arunachal Pradesh, India, and its palaeoclimatic significance. Palaeobiol. Palaeoenvol. 91, 237–255.
Knorr, G., Butzin, M., Micheels, A., Lohmann, G., 2011. A warm Miocene climate at low atmospheric CO_2 levels. Geophys. Res. Lett. 38, L20701.
Lei, Y.L., Zhong, D.L., Jia, C.Z., Ji, J.Q., Zhang, J., 2008. Late Cenozoic differential uplift–exhumation of batholith and propagation of uplift recorded by fission track thermochronology in Chayu area, the east margin of Tibetan plateau. Acta Petrol. Sin. 24, 384–394 (in Chinese with English abstract).
Leng, Q., 1999. Analysis on the classification of deciduous Fagaceae from China based on leaf architecture. Palaeoworld 12, 65–84.
Li, H.M., Guo, S.X., 1982. Seed plants. In: Nanjing Institute of Geology and Mineral Resources (Ed.), Palaeotological Atlas of East ChinaMesozoic and Cenozoic Era vol. 3. Geological Publishing House, Beijing, pp. 280–316 (in Chinese).
Liu, M.Q., 2010. Leaf Cuticle, Architecture, Embryology and Biogeography of *Castanopsis* (D.Don) Spach and Related Genera (Fagaceae) (Ph.D. Dissertation) Kunming Institute of Botany, Chinese Academy of Sciences (in Chinese with English abstract).
Luo, Y., 2000. Leaf Epidermis, Leaf Architecture, Phytogeography and Phylogeny of *Quercus* Subgenus *Cyclobalanopsis* (Oerst.) Scheneid. From China (MS.D. dissertation) Kunming Institute of Botany, Chinese Academy of Sciences (in Chinese with English abstract).
Luo, Y., Zhou, Z.K., 2001. Phytogeography of *Quercus* subgenus *Cyclobalanopsis*. Acta Bot. Yunnan 23 (1), 1–16 (in Chinese, with English Abstract).
Luo, Y., Zhou, Z.K., 2002. Leaf architecture in *Quercus* subgenus *Cyclobalanopsis* (Fagaceae) from China. Bot. J. Linn. Soc. 140 (3), 283–295.
Ma, H.J., Zhang, S.T., Su, T., Wang, L., Sui, S.G., 2012. New materials of *Eguisetum* from the Upper Miocene of Mangkang, eastern Xizang and its ecological implications. J. Jilin Univ. (Earth Sci. Ed.) 42, 189–195 (in Chinese, with English Abstract).
Meng, J., Wang, C.S., Zhao, X.X., Coe, R., Li, Y.L., Finn, D., 2012. India–Asia collision was at 24 °N and 50 Ma: palaeomagnetic proof from southernmost Asia. Sci. Rep. 2, 925.
Miao, Y.F., Herrmann, M., Wu, F.L., Yan, X.L., Yang, S.L., 2012. What controlled Mid-Late Miocene long-term aridification in Central Asia? Global cooling or Tibetan Plateau uplift: a review. Earth-Sci. Rev. 112, 155–172.
Micheels, A., Bruch, A.A., Uhl, D., Utescher, T., Mosbrugger, V., 2007. A Late Miocene climate model simulation with ECHAM4/ML and its quantitative validation with terrestrial proxy data. Palaeogeogr. Palaeoclimatol. Palaeoecol. 253, 251–270.
Molnar, P., England, P., Martinod, J., 1993. Mantle dynamics, uplift of the Tibetan Plateau and the Indian monsoon. Rev. Geophys. 31, 357–396.
Molnar, P., Boos, W.R., Battisti, D.S., 2010. Orographic controls on climate and paleoclimate of Asia: thermal and mechanical roles for the Tibetan Plateau. Annu. Rev. Earth Planet. Sci. 38, 77–102.
Mosbrugger, V., Utescher, T., 1997. The coexistence approach—a method for quantitative reconstructions of Tertiary terrestrial palaeoclimate data using plant fossils. Palaeogeogr. Palaeoclimatol. Palaeoecol. 134, 61–86.
Pound, M.J., Haywood, A.M., Salzmann, U., Riding, J.B., Lunt, D.J., Hunter, S.J., 2011. A Tortonian (Late Miocene, 11.6–7.25 Ma) global vegetation reconstruction. Palaeogeogr. Palaeoclimatol. Palaeoecol. 300, 29–45.
Raymo, M.E., Ruddiman, W.F., 1992. Tectonic forcing of Late Cenozoic climate. Nature 359, 117–122.
Rowley, D.B., 1996. Age of initiation of collision between India and Asia: a review of stratigraphic data. Earth Planet. Sci. Lett. 145, 1–13.
Rowley, D.B., Currie, B.S., 2006. Palaeo-altimetry of the late Eocene to Miocene Lunpola basin, central Tibet. Nature 439, 677–681.
Royden, L.H., Burchfiel, B.C., van der Hilst, R.D., 2008. The geological evolution of the Tibetan Plateau. Science 321, 1054–1058.
Schoenbohm, L.M., Burchfiel, B.C., Chen, L.Z., 2006. Propagation of surface uplift, lower crustal flow, and Cenozoic tectonics of the southeast margin of the Tibetan Plateau. Geology 34, 813–816.
Soepadmo, E., 1972. Fagaceae. In: van Steenis, C.G.G.J. (Ed.), Flora Malesiana Series ISeed Plants vol. 7 (2). Noordhoff-Kolff n.v., Djakarta, pp. 386–387.
Song, X.Y., Spicer, R.A., Yang, J., Yao, Y.F., Li, C.S., 2010. Pollen evidence for an Eocene to Miocene elevation of central southern Tibet predating the rise of the High Himalaya. Palaeogeogr. Palaeoclimatol. Palaeoecol. 297, 159–168.
Spicer, R.A., Harris, N.B.W., Widdowson, M., Herman, A.B., Guo, S.X., Valdes, P.J., Wolfe, J.A., Kelley, S.P., 2003. Constant elevation of southern Tibet over the past 15 million years. Nature 421, 622–624.
Su, T., 2010. On the Establishment of the Leaf Physiognomy–Climate Model and A Study of the Late Pliocene Yangjie Flora, Southwest China (Ph.D. Dissertation) University of the Chinese Academy of Sciences (in Chinese with English abstract).
Su, T., Wilf, P., Xu, H., Zhou, Z.K., 2014. Miocene leaves of *Elaeagnus* (Elaeagnaceae) from the Qinghai–Tibet Plateau, its modern center of diversity and endemism. Am. J. Bot. 101 (8), 1350–1361.
Sun, B., Wang, Y.F., Li, C.S., Yang, J., Li, J.F., Li, Y.L., Deng, T., Wang, S.Q., Zhao, M., Spicer, R.A., Ferguson, D.K., Mehrotra, R.C., 2015. Early Miocene elevation in northern Tibet estimated by palaeobotanical evidence. Sci. Rep. 5, 10379.
Tanai, T., 1953. Notes on some plant fossils from Ennichi (Yongil) group in southern Korea, II. Trans. Proc. Paleontol. Soc. Jpn. N. Ser. 9, 1–7.
Tanai, T., 1995. Fagaceae leaves from the Paleocene of Hokkoiado, Japan. Bull. Natl. Sci. Mus. C Geol. Paleontol. 21 (3/4), 71–101.
Tang, H., Micheels, A., Eronen, J.T., Ahrens, B., Fortelius, M., 2013. Asynchronous responses of East Asian and Indian summer monsoons to mountain uplift shown by regional climate modelling experiments. Clim. Dyn. 40, 1531–1549.
Tao, J.R., 2000. The Evolution of the Late Cretaceous–Cenozoic Flora in China 282. Science Press, Beijing (in Chinese).
Tao, J.R., Chen, M.H., 1983. Cenozoic flora of Lincang. In: Team of Comprehensive Scientific Expedition to the Qinghai–Xizang Plateau, Chinese Academy of Sciences (Ed.), Studies in Qinghai–Xizang Plateau — Special Issue of Hengduan Mountains Scientific Expedition (I). Yunnan People's Publishing House, Kuming, pp. 74–95 (in Chinese).
Tao, J.R., Du, N.Q., 1987. Miocene flora from Markam County and fossil record of Betulaceae. Acta Bot. Sin. 29, 649–655 (in Chinese with English abstract).
Tao, J.R., Kong, Z.C., 1973. The fossil florule and sporo-pollen assemblage of the Shang-In Coal series of Erhyuan, Yunnan. Acta Bot. Sin. 15, 120–126 (in Chinese with English abstract).
Tapponnier, P., Xu, Z.Q., Roger, F., Meyer, B., Arnaud, N., Wittlinger, G., Yang, J.S., 2001. Oblique stepwise rise and growth of the Tibet Plateau. Science 294, 1671–1677.
Tiffney, B.H., Manchester, S.R., 2001. The use of geological and paleontological evidence in evaluating plant phylogeographic hypotheses in the northern hemisphere Tertiary. Int. J. Plant Sci. 162, S3–S17.
Wang, Q., Spicer, R.A., Yang, J., Wang, Y.F., Li, C.S., 2013. The Eocene climate of China, the early elevation of the Tibetan Plateau and the onset of the Asian Monsoon. Glob. Chang. Biol. 19, 3709–3728.
Wang, C.S., Dai, J.G., Zhao, X.X., Li, Y.L., Graham, S.A., He, D.F., Ran, B., Meng, J., 2014. Outward-growth of the Tibetan Plateau during the Cenozoic: a review. Tectonophysics. 621, 1–43.
Wen, W.W., 2011. Nine Fossil Plants of Fagaceae from the Pliocene in Baoshan, Yunnan and Paleoenvironmental Analysis (MS.D. Dissertation) College of Earth and Environmental Sciences, Lanzhou University (in Chinese with English abstract).
Westaway, R., 2009. Active crustal deformation beyond the SE margin of the Tibetan Plateau: constraints from the evolution of fluvial systems. Glob. Planet. Chang. 68, 395–417.
Wing, S.L., Greenwood, D.R., 1993. Fossils and fossil climate: the case for equable continental interiors in the Eocene. Philos. Trans. R. Soc. B 341, 243–252.
Wolfe, J.A., 1995. Paleoclimatic estimates from Tertiary leaf assemblages. Annu. Rev. Earth Planet. Sci. 23, 119–142.
Woodward, F.I., 1987. Climate and Plant Distribution. Cambridge University Press, Cambridge.
Writing Group of Cenozoic Plants of China (WGCPC), 1978. Cenozoic Plants From China, Fossil Plants of China vol. 3. Science Press, Beijing (in Chinese).
Wu, Y.H., 2008. The Vascular Plants and Their Eco-geographical Distribution of the Qinghai–Tibetan Plateau. Science Press (in Chinese).
Wu, J.Y., 2009. The Pliocene Tuantian Flora of Tengchong, Yunnan Province and Its Paleoenvironmental Analysis (Ph.D. Dissertation) Lanzhou University (in Chinese with English abstract).
Wu, Z.H., Barosh, P.J., Wu, Z.H., Hu, D.G., Zhao, X., Ye, P.S., 2008. Vast early Miocene lakes of the central Tibetan Plateau. Geol. Soc. Am. Bull. 120 (9–10), 1326–1337.
Xia, K., Su, T., Liu, Y.S.C., Xing, Y.W., Jacques, F.M.B., Zhou, Z.K., 2009. Quantitative climate reconstructions of the late Miocene Xiaolongtan megaflora from Yunnan, southwest China. Palaeogeogr. Palaeoclimatol. Palaeoecol. 276, 80–86.
Xing, Y.W., 2010. The Late Miocene Xianfeng Flora, Yunnan, Southwest China and its Quantitative Palaeoclimatic Reconstructions (Ph.D. Thesis) Kunming Institute of Botany, Chinese Academy of Sciences, Kunming, China (in Chinese, with English Abstract).
Xing, Y.W., Utescher, T., Jacques, F.M.B., Su, T., Liu, Y.S.C., Huang, Y.J., Zhou, Z.K., 2012. Palaeoclimatic reconstructions reveal weak precipitation seasonality in southwestern China during the late Miocene: evidence from plant macrofossils. Palaeogeogr. Palaeoclimatol. Palaeoecol. 358–360, 19–26.
Xing, Y.W., Hu, J.J., Jacques, F.M.B., Wang, L., Su, T., Huang, Y.J., Liu, Y.S., Zhou, Z.K., 2013. A new *Quercus* species from the upper Miocen of southwestern China and its ecological significance. Rev. Palaeobot. Palynol. 193, 99–109.
Xu, R., Tao, J.R., Sun, X.J., 1973. On the discovery of a *Quercus semicarpifolia* bed in mount Shisha Pangma and its significance in botany and geology. Acta Bot. Sin. 15 (1), 103–119 (in Chinese with English abstract).
Yao, Y.F., Bruch, A.A., Mosbrugger, V., Li, C.S., 2011. Quantitative reconstruction of Miocene climate patterns and evolution in Southern China based on plant fossils. Palaeogeogr. Palaeoclimatol. Palaeoecol. 304, 291–307.
Yun, F., 2007. Research on Cuticles of Five Fossil Plants From Pliocene in Tengchong of Yunnan (Ph.D. Dissertation) Lanzhou University (in Chinese with English abstract).
Zachos, J.C., Dickens, G.R., Zeebe, R.E., 2008. An early Cenozoic perspective on greenhouse warming and carbon-cycle dynamics. Nature 451, 279–283.
Zhang, J.H., 1978. Paleobotany. In: Team of Stratigraphy Palaeontology (Ed.), Atlas of Palaeontology of Southwest China, Guizhou Volume (II). Geological Publishing House, Beijing, pp. 480–490 (in Chinese).

Zhang, J.W., Chen, W.L., Zhao, K.Y., Wang, J.T., Li, B.S., 1988. Vegetation partition. In: Team of Comprehensive Scientific Expedition to the Qinghai–Xizang Plateau, Chinese Academy of Sciences (Ed.), Vegetation of Xizang (Tibet). Science Press, Beijing, pp. 283–284 (in Chinese).

Zhang, P.Z., Shen, Z.K., Wang, M., Gan, W.J., Bürgmann, R., Molnar, P., Wang, Q., Niu, Z.J., Sun, J.Z., Wu, J.C., Sun, H.R., You, X.Z., 2004. Continuous deformation of the Tibetan Plateau from global positioning system data. Geology 32 (9), 809–812.

Zhang, Q.H., Willems, H., Ding, L., Gräfe, K.U., Appel, E., 2012. Initial India–Asia continental collision and foreland basin evolution in the Tethyan Himalaya of Tibet: evidence from stratigraphy and paleontology. J. Geol. 120, 175–189.

Zhou, Z.K., 1985. The Miocene Xiaolongtan Fossil Flora in Kaiyuan, Yunnan, China (M.Sc. Thesis) Nanjing Institute of Geology and Palaeontology, Chinese Academy of Sciences, Nanjing, China (in Chinese).

Zhou, Z.K., 1993. The fossil history of *Quercus*. Acta Bot. Yunnan 15 (1), 21–33 (in Chinese, with English Abstract).

Zhou, Z.K., 1996. Studies on *Dryophyllum* complex from China and its geological and systematic implications. Acta Bot. Sin. 38 (8), 666–671 (in Chinese, with English Abstract).

Zhou, Z.K., 2000. On the Miocene Xiaolongtan flora from Kaiyuan, Yunnan Province. In: Tao, J.R. (Ed.), The Evolution of the Late Cretaceous–Cenozoic Floras in China. Science Press, Beijing, pp. 64–72 (in Chinese).

Zhou, Z.K., Wilkinson, H., Wu, Z.Y., 1995. Taxonomical and evolutionary implications of the leaf anatomy and architecture of *Quercus* L. subgenus *Quercus* from China. Cathaya 7, 1–34.

Zhou, Z.K., Yang, Q.S., Xia, K., 2007. Fossils of *Quercus* sect. *Heterobalanus* can help explain the uplift of the Himalayas. Chin. Sci. Bull. 52 (2), 238–247 (in Chinese).